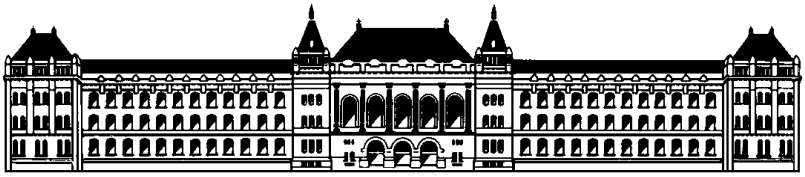

University of Technology and Economics
Faculty of Mechanical Engineering
Department of Hydrodynamic Systems

Application of non-Newtonian liquids in automotive control systems

Booklet of PhD dissertation

Written by: Péter Nagy-György
mechanical modelling engineer

Supervisor: Dr. Csaba Hős
associate professor

Budapest, April 6, 2022

1 Introduction

Truck systems have several worn parts whose erosion need to be compensated for over the vehicle's lifetime, e.g. brake wear, valve lash, clutch disc wear. The present dissertation seeks a solution to compensate for the wear and tear modifications of clutch discs in transmission systems.

Several attempts have been made to compensate for the variation of the dead volume (to compensate the wear and keep the actuator-piston at the same level in the released state) since a successful design would have a significant market advantage: operating range can be held at the end of the cylinder to minimize the dead volume (better dynamics), and the cylinder can be smaller as the stroke does not have to cover the wear (space and cost savings). Active solutions work by controlling electrical devices (e.g. solenoid valves), but the cost of the proper control is high. Mechanical solutions are usually based on friction. If the force unbalances due to the dead volume change exceeding the friction force, then the length of the adjuster changes [1, 2]. The efficiency depends on the precise tune of the friction that controls the adjustment, which is costly due to sufficiently precise surface machining.

A common requirement of the above-presented actuators is that they *should be rigid during high load (e.g. braking, clutch depression) while in the steady-state (after braking, clutch closed), it should change length due to the small unbalances.* Typical brake actuators usually compensate only in one direction. Hydraulic valve lash adjusters also only perform unidirectional adjustment (so they are inappropriate to balance the thermal expansion in the opposite direction). Friction clutch adjusters require costly surface machining due to the above-presented reasons. Therefore, colossal demand rises for a reliable but inexpensive adjuster that is rigid under high loads and flexible under small loads.

Satisfying the demand drove the interest toward the idea of a shear thickening fluid-based adjuster. These fluids have low viscosity and can flow by low shear rates (and shear stress), while at high shear rates (and shear stress), they have high viscosity and can even behave like solids. The patented idea from Knorr-Bremse Brake Systems Ltd. is similar to a single-tube shock absorber where the chambers are filled with a shear thickening fluid. According to the patent, the chambers are connected by a channel with a circular cross-section, in which the fluid can flow due to the pressure difference between the chambers. The proper fluid (and thus the adjuster) hardens during actuation while in the released state, the liquid softens at low forces, and the adjuster becomes flexible. The research aims to conduct a feasibility study, select the fluid, and design the device. Hopefully, the resulting device will have fewer components, less stringent tolerances, surface machining, and thus lower cost.

1.1 Research plan

The research aims to build up a non-Newtonian fluid-based adjuster. The device would be mounted in the rod of the clutch actuator in the automatic transmission system of heavy vehicles, and its function is to compensate for length variations (e.g. due to wear, thermal

expansion) that occur during the lifetime. The adjuster must satisfy two requirements: a) be sufficiently rigid during high load and fast actuation, and b) be sufficiently flexible in the released state to compensate for length variations and compression during actuation.

The solution of the problem started with the description of the non-Newtonian flow in the channel. An analytical method is built up to determine the volume flow rate - pressure drop characteristic curve of the channel for an arbitrary non-Newtonian liquid assuming laminar flow not only for an annular but also for a circular hole cross-section channel. The method can be employed to predict the behaviour of the adjuster by determining the speed of compression (and the corresponding volume flow rate) for a given force (and pressure difference). The method can also be applied to determine the damping characteristics of a non-Newtonian fluid-based shock absorber. A graphical representation has been worked out for the analytical derivation, which is well suited for industrial application. Based on the methods, Thesis I. is stated.

In order to validate the models, more accurate but computationally demanding simulations were performed with several types of shear thickening liquids for annular and cylindrical hole gaps. The simulation results were exploited to define the dimensionless range of the geometrical dimensions, where the error due to the simplifications is within acceptable range. The description of the analytical methods with the acceptable parameter space forms Thesis II.

The simplified models are validated not only by more accurate CFD simulations but also by experiments. I have assembled a test rig to measure the compression of an adjuster filled with different liquids under the actuator's load. The measurements were performed for Newtonian (hydraulic oil), traditional non-Newtonian (silicone oil - Cross-model) and complex shear thickening fluids. The latter was prepared, and its rheological properties were measured by the Soft Materials Research Group of the Faculty of Chemical Engineering, BME. The rheological measurement results were directly inserted into the simplified models. The analytical values showed reasonable agreement with the experimental results.

The main role of the simplified analytical model is to describe the effect of the non-Newtonian rheology on the adjuster's behaviour with acceptable accuracy and low computational cost. The main advantage of the model is that it can use the results of the rheological measurements directly for arbitrary rheology; hence, any rheological model fitting is unnecessary. However, the main disadvantage of the model is that it applies a quasi-stationary approximation, so it gives acceptable results only for slow processes. Therefore, additional transient simulations were performed to define the acceptance criterion for the quasi-stationary approximation for a power-law liquid. This result constitutes Thesis III.

The behaviour of the adjuster device was described by means of equations of motion written for the moving parts. The flow model mentioned above couples the equations corresponding to the different bodies. Based on the system of ordinary differential equations, multi-objective optimization is performed to calculate the dimensions of the device using different fluid rheologies from the literature. The two objective functions of the optimization are a) the compression during actuation and b) the length of the uncompensated wear during the released state. The results showed that two fluids have size combinations that

meet the requirements of the industrial partner. Further transient CFD simulations also verify the selected combinations. The design guidelines based on the evaluation of the results contribute to my Thesis IV.

In summary, a patented non-Newtonian fluid-based device is designed based on the developed mathematical models, and more accurate steady-state and transient numerical computations (CFD) and measurements verify its accuracy. The developed numerical toolbox provides a reasonable basis for further development of the shear thickening liquids from the chemical engineering point of view.

2 Analytical models for non-Newtonian fluid flow

In shock absorbers, the fluid typically flows through two types of flow restriction: a cylindrical hole (usually for hydraulic fluid, 2) and a circular annular gap (e.g. for magnetorheological fluid, 1). Thus, these two types of gaps are investigated.

In both cases, the piston (a1, c1) in a cylinder (a2, c2) moves due to the external compressive or tensile forces. A pressure difference builds up between chambers (a3,c3) and (a5, c5), causing the fluid flow from the pressurised chamber to the lower pressure chamber through the flow restriction (a4, c4). In the case of the annular gap, the gap is bordered by the bore in the piston and the circular rod fixed to the cylinder. In both cases, the fluid is sealed (a6, c6).

The behaviour of the shock absorber or a similarly structured adjuster is characterised by the relationship between the compression force F and the compression velocity v, as confirmed by the measurement results. The viscous flow force acting on the piston can be calculated as the product of the pressure difference between the chambers and the piston surface area, while the piston rod velocity is obtained as the ratio of the volume flow rate and the piston surface area. In order to determine the relationship $F(v)$, it is essential to determine the characteristic curve of the flow restriction $\Delta p(Q)$ for the applied incompressible non-Newtonian fluid. The challenge of the present application is that the rheological behaviour of the fluid can be quite complex.

The characteristic curves have been determined for both annular and hole-shaped gaps; however, only the main steps of the former derivation are presented in this section.

2.1 Determination of the pressure difference - volume flow rate curve analytically and graphically

The mean diameter of the gap is assumed to be much larger than the size of the gap, so the gap flow is approximated by the flow between parallel plates. The solution is derived from the continuity and momentum equation written in the Cartesian coordinate system, assuming an incompressible medium. The following assumptions are made to obtain the analytical solution: 1) the fluid is incompressible, 2) steady-state, no time dependence, 3) the flow is two dimensional, so all quantities are constant in the z direction, 4) the velocity in the x (streamwise) direction depends only on the y (spanwise) coordinate ($u = u(y)$),

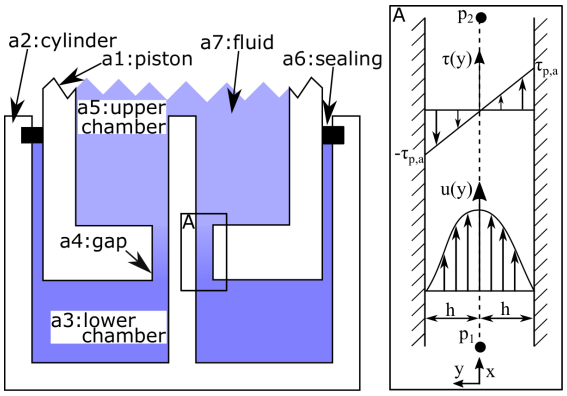

Figure 1: Schematic diagram of a non-Newtonian fluid-filled adjuster/shock absorber with an annular gap.

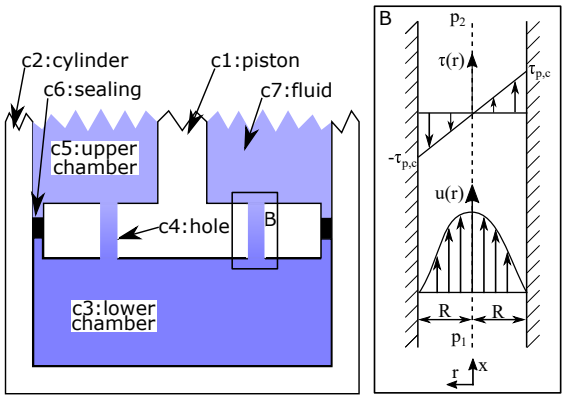

Figure 2: Schematic diagram of a non-Newtonian fluid-filled adjuster/shock absorber with the circular hole.

the other velocity components are zero $v = w = 0$ and 4) the pressure gradient is constant $dp/dx = const$. Under these conditions, the continuity and the momentum equation in the y and z directions are automatically satisfied. (Similar train of thought can be found in the literature [3], which results have been validated by measurement [4]). The remaining simplified equation is

$$0 = -\frac{dp}{dx} + \frac{d\tau}{dy}, \tag{1}$$

where $\tau(y)$ is the local shear stress. Integrating the equation with respect of y from $y = 0$ (the axis of the channel, see Figure 1), the form of

$$\tau = -\frac{dp}{dx}y + \tau_0, \tag{2}$$

is obtained for the local shear stress, where $\tau_0 = \tau(0)$ is the local shear stress at the channel's centerline. The goal is to determine the velocity profile and the volume flow rate for a given pressure gradient and rheology. The velocity is represented in the rheology model since the shear stress is a function of the shear rate in some $\tau = g(\dot{\gamma} = \frac{du}{dy})$. So, according to the traditional method, the next step is to express the shear rate $\dot{\gamma} = \frac{du}{dy}$ from the equation (2). This is still feasible in closed form for simpler non-Newtonian models, such as the Bingham, power-law and Herschel-Bulkley models, since the shear rate can be explicitly computed from the shear stress.

In the present paper, we investigate the complex shear thickening fluid in industrial applications for which no simple rheological model exists. Moreover, at the initial design stage, it is unknown whether any fluid would be suitable for the application (typically characterised by a prescribed $F(v)$ function). For this reason, a novel method is developed to determine the volume flow rate - pressure difference curve for arbitrary rheology. The inputs of the method are the rheology of the fluid $\tau = g(\dot{\gamma})$, the dimensions of the gap (L length, h half-height, W width) and the wall velocity u_w, while the output is the characteristic curve $Q(\Delta p)$. The steps of the solution are the following:

1. Determine the inverse rheological curve $f(\tau) = \dot{\gamma} = g^{-1}(\tau)$ from the rheological measurement results $\tau = g(\dot{\gamma})$
2. Odd extension $f_{odd}(\tau)$ of the curve $f(\tau)$
3. Produce the first $F_{odd}(\tau)$ integral function of $f_{odd}(\tau)$,
4. Produce the second $S_{odd}(\tau)$ integral function of $f_{odd}(\tau)$,
5. Determination of τ_0 satisfying the boundary conditions using equation

$$F_{odd}(\tau_0 - \tau_p) - F_{odd}(\tau_0 + \tau_p) = \frac{u_w \tau_p}{h} \tag{3}$$

6. Determination of the characteristic curve $Q(\Delta p)$ using equation

$$\frac{Q}{W} = \frac{h^2}{\tau_p^2} \left[2\tau_P F_{odd}(\tau_0 - \tau_p) + S_{odd}(\tau_0 - \tau_p) - S_{odd}(\tau_0 + \tau_p) \right]. \tag{4}$$

The advantage of this method is that steps 2 and 3 can be performed using some numerical method (e.g. trapezoidal method) from the measurement results directly without any model fitting.

In order to prove the validity of the derivation, the method was verified with measurement data obtained from the literature (tape casting with Bingham fluid [5], shear thickening fluid-based shock absorber [6]) and CFD.

To improve the industrial applicability, a graphical method is developed to define the velocity profile and the characteristic curve graphically, even using a simple spreadsheet software. If the rheological measurement data have sufficiently fine resolution, the function F_{odd} can be produced by numerical integration of the measurement data (e.g. by the trapezoidal method). Then the function S_{odd} can also be plotted after another numerical integration. The τ_0 solution of the eqution(3) can also be obtained graphically: find the "window" of width $2\tau_P$ and height $\frac{u_w \tau_p}{h}$ (as shown in Figure T1 b) where τ_p is defined by the equation (2). Let $F_A = F_{odd}(\tau_0 - \tau_p)$ and $F_B = F_{odd}(\tau_0 + \tau_p)$. Then, if $u_w > 0$ then $F_B > F_A$ and vice versa, so the assignment is straightforward, even though the function $F_{odd}(\tau)$ is even. After reading the corresponding points F_A, F_B, S_A and S_B (see Figure T4) we have

$$\frac{Q(\tau_p, u_w)}{W} = \frac{h^2}{\tau_P^2} \left(2\tau_P F_B + S_A - S_B \right). \tag{5}$$

Thesis 1

A novel graphical method is developed to determine the characteristic curve $Q(\Delta p, u_w)$ for laminar Couette-Poiseuille flow of a fluid with arbitrary rheology $\tau = g(\dot{\gamma})$, where Q is the volume flow rate through the gap, Δp is the pressure difference, and u_w is the moving wall velocity; the gap width is h and length is L. The steps of the method are the following:

1. Draw the inverse rheological curve $f(\tau) = \dot{\gamma} = g^{-1}(\tau)$ from the rheological measurement results $\tau = g(\dot{\gamma})$,

2. create odd extension $f_{odd}(\tau)$ in negative region of the curve $f(\tau)$.

3. produce the first $F_{odd}(\tau)$ and second $S_{odd}(\tau)$ integral curve of the function $f_{odd}(\tau)$,

4. adjust the window with $2\tau_P$ width and $\frac{|u_w|\tau_P}{h}$ height on the plotted $F_{odd}(\tau)$ function, where $\tau_P = \frac{\Delta p}{L}h$, Δp is the pressure difference through the gap, h is the gap's halfwidth, L is the length of the gap and u_w is the moving wall velocity,

5. read the points F_B, S_A, S_B from the graph (see figure), finally

6. substitute into equation

$$Q(\Delta p, u_w) = \frac{Wh^2}{\tau_P^2}\left(2\tau_P F_B + S_A - S_B\right).$$

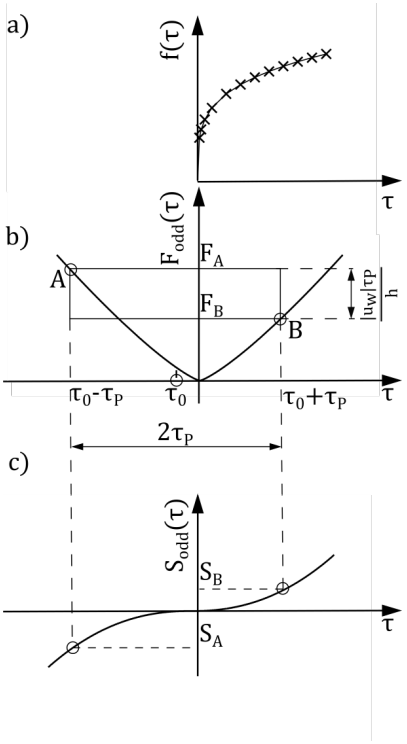

Figure T1. The graphical method to determine the volume flow rate for a given pressure gradient and wall velocty.

Related publication: [J1].

2.2 Application to model shock absorbers

In a real design, the piston surface of a shock absorber can be several orders of magnitude larger than the cross-section of the gaps, see Figure 1. In this case, the piston wall velocity is negligible compared to the average flow velocity in the gap. Omitting the wall velocity simplifies the derivation of the previous section since the flow between stationary walls (pure Poiseuille flow) is symmetric, so the shear stress on the axis of symmetry is zero $\tau_0 = 0$. Then the expression for the volumetric flow rate is simplified to the following form

$$Q = \frac{Wh^2}{{\tau_P}^2}[2\tau_P F_{odd}(\tau_P) - 2S_{odd}(\tau_P)]. \tag{6}$$

Then there is no need to solve the (3) nonlinear equation and the characteristic curve $Q(\Delta p)$ can be obtained directly by numerical integration. Let us define the relative volumetric flow rate $\tilde{Q}$ by dividing the volume flow rate with the term of Wh^2

$$\tilde{Q} := \frac{Q}{Wh^2} = \frac{1}{{\tau_P}^2}[2\tau_P F_{odd}(\tau_P) - 2S_{odd}(\tau_P)]. \tag{7}$$

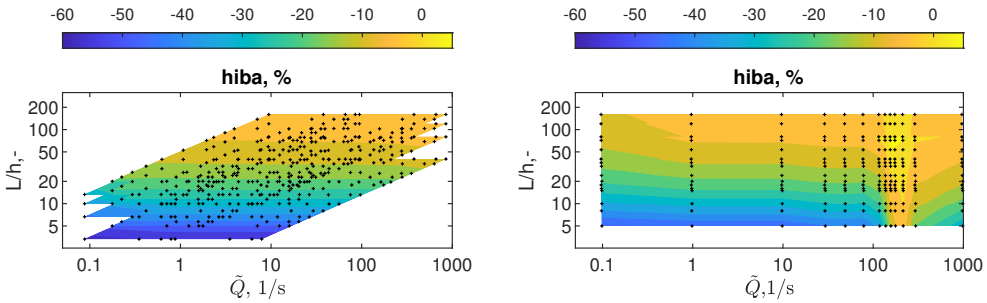

Figure 3: Relative error of the analytical model compared to the CFD results for power law (left) and shear thickening fluid (right) in the case of annular gap. The results show that the relative error depends on the relative gap length for a power law fluid and on the relative gap length and the relative volume flow rate for a shear thickening fluid.

It can then be observed that the left-hand side of the equation depends only on the inverse rheology f and its first and second integral functions. The curve $\tilde{Q}(\tau_P)$ can be produced for given rheology without knowing the dimensions of the flow restriction. If the dimensions of the damper are known, the damping characteristic $F(v)$ can be obtained from equation

$$v = \frac{Q}{A} = \frac{\tilde{Q}Wh^2}{A} \quad \text{and} \quad F = \Delta pA = \tau_P \frac{L}{h} A. \tag{8}$$

Since both the velocity and the force are multiplied by a geometry-dependent constant, the shape of the curve $F(v)$ does not change but only stretches along the x and y axes. This allows us to state that the shape of the damping characteristic depends only on the rheology. For example, a shear thinning fluid is appropriate for degressive power-law damping, while progressive damping can be achieved with a shear thickening liquid. If the shear thickening fluid has a thinning region, degressive damping can also be reached with a proper design.

There are only a few well-documented measurements in the literature, so the analytical model results could only be validated over a narrow range of dimensions. Therefore, to estimate the error of the analytical models, I performed parameter sweeps for both geometries by means of CFD (Computational Fluid Dynamics). For the annular gap, the length L of the gap (L=2.5; 5; 7.5; 10 mm) and the inner diameter d_i (d_i=5.75; 5.44; 4.75; 4 mm) were varied by different inlet velocity. The relative error of the pressure difference values obtained analytically and numerically (CFD) are compared in the function of the relative gap size $\frac{2h}{d_i+d_o}$ and the dimensionless gap length $L/h$for power-law (PL) and shear thickening fluid (STF).

A comparison of the analytical and CFD results of the parameter sweep is shown in Figure 3 for an annular gap. The upper panels show the relative error of the results obtained with different relative gap sizes $\frac{2h}{d_i+d_o}$ in the plane $L/h - \tilde{Q}$. The black dots represent the dimension combinations tested by CFD, so the plots show the relative error values at these points. In the case of a power-law fluid (left column), the contour lines are nearly horizontal, so the effect of the volume flow rate is negligible compared to the relative gap length L/h.

The arbitrarily chosen maximum allowable relative error of 10% for both fluids is guaranteed by the condition $L/h > 100$. The numerical tests were repeated with a circular hole case by varying the diameter d and the length L. In this case, the maximum relative error condition of 10% must be satisfied by $L/D > 10$ criterium.

Thesis 2

A single-tube piston damper with nonlinear damping characteristics can be designed using shear thickening fluid. If the fluid rheology includes thinning and thickening regions as well, progressive and degressive damping characteristics can also be achieved depending on the size of the flow restriction. Relationship between the velocity damping characteristic of the single-tube damper $v(F)$ and the rheology of the fluid $f(\tau) := \dot{\gamma}(\tau)$ can be described by

- for *annular gap*

$$v = \frac{a}{(bF)^2}\left(2bF\int_0^{bF} f(\tau)\,d\tau - \int_0^{bF} F(\tau)\,d\tau\right), \quad \text{where} \qquad a = \frac{Wh^2}{A_p}, \quad b = \frac{h}{A_pL},$$

- while for *circular hole*

$$v = \frac{c}{(dF)^2}\left(2dF\int_0^{dF} f(\tau)\,d\tau - \int_0^{dF} \tau F(\tau)\,d\tau\right), \quad \text{where} \qquad c = \frac{2\pi R^3}{A_p}, \quad d = \frac{R}{2A_pL}$$

and $\quad F = \int f(\tau)\,d\tau.$

equations. Compared to CFD calculations, the applicability range of the method with a 10% error limit is $L/h > 100$ for an annular gap and $L/D > 10$ for a cylindrical hole.

In the above presented formulas, v is the velocity, F is the the damping force, and a, b, c, d are geometrically dependent constants. The dimensions of the annular gap are the circumference W and h halfwidth. R is the radius of the hole. In both cases, L is the length of the gap and A_p is the piston surface. The inverse rheological curve of the liquid is $\dot{\gamma} := f(\tau)$.

Related publications: [J2], [C2], [C3].

3 Transient studies

In the previous chapter, the actual dynamic process was approximated by a series of equilibria, so the question may arise: under what conditions is this approximation valid? In vibration dampers, the hysteresis phenomenon can often occur at high frequencies, when the damping characteristic $F(v)$ depends significantly on the excitation frequency. In such cases, the $F(v)$ characteristic is not a single curve but a loop, and the area inside the loop expands with increasing frequency, see [7].

To describe the time-dependent dynamics of the Couette-Poiseuille flow, semi-analytical models are available in the literature, such as [8] for Newtonian, [9] for Bingham and [10] for Herschel-Bulkley fluids. The authors found that the difference between the quasi-stationary and unsteady solutions in phase shift and amplitude can be significant in certain parameter ranges. However, they did not define critical parameter values beyond which the quasi-stationary solution is not sufficiently accurate.

The present chapter defines the range of acceptability of the quasi-stationary approximation for a non-Newtonian fluid. Since the time-dependent flow equations have an analytical solution in the linear (Newtonian) case, this was the starting point. Based on the derivation, I established the relationship between the coefficients of the harmonic pressure difference and volume flow rate functions using dimensionless quantities. From the relation, the range could be determined where the pressure difference and volume flow rate functions are in nearly the same phase.

The analytical solution was compared to the results of the transient numerical CFD simulations to verify the accuracy of the numerical solutions. In the case of power-law fluid, the governing equations were solved employing the CFD technique. Based on the results, the criteria defined for the Newtonian case have been extended to the non-Newtonian case. Based on the results, I formulated my Thesis III.

3.1 Result of the Newtonian derivation

In the Newtonian case, the time-dependent form of the equation of motion is

$$\rho\frac{\partial u(y,t)}{\partial t} = -\frac{dp}{dx} + \mu\frac{\partial^2 u(y,t)}{\partial y^2}, \quad u(-h,t) = 0, \quad u(h,t) = v(t), \tag{9}$$

where u is y spanwise coordinate dependent velocity in the gap, x direction and μ is the dynamic viscosity. The velocity of the wall is the ratio of the volumetric flow rate and the piston area $v(t) = Q(t)/A$. If the dimensionless volumetric flow rate

$$\hat{q} = c_{CP}\cos(\hat{t}St) + d_{CP}\sin(\hat{t}St) \tag{10}$$

and dimensionless pressure difference

$$\hat{p_x} = a\cos(\hat{t}St) + b\sin(\hat{t}St) \tag{11}$$

are harmonic functions, then the relatinship between a, b, c_{CP} and d_{CP} coefficients can be expressed by the equation

$$\left(I - \frac{Wh}{A}\begin{bmatrix} C_{11}(Wo) & C_{12}(Wo) \\ -C_{12}(Wo) & C_{11}(Wo) \end{bmatrix}\right)\begin{bmatrix} c_{CP} \\ d_{CP} \end{bmatrix} = \frac{4}{Wo^2}\begin{bmatrix} -C_{12}(Wo) & C_{11}(Wo)-1 \\ C_{11}(Wo)-1 & C_{12}(Wo) \end{bmatrix}\begin{bmatrix} a \\ b \end{bmatrix}, \tag{12}$$

where C_{11} and C_{12} are constants depend on the Womersley number Wo

$$C_{11} = \frac{1}{Wo}\frac{\sin(Wo)+\sinh(Wo)}{\cos(Wo)+\cosh(Wo)} \quad C_{12} = \frac{1}{Wo}\frac{\sin(Wo)-\sinh(Wo)}{\cos(Wo)+\cosh(Wo)}. \tag{13}$$

The constants in the equations are the Womersley number $Wo = \sqrt{2StRe}$, the Strouhal number $St = \frac{\omega h}{U}$ and the Reynolds number $Re = \frac{\rho U h}{\mu}$. Based on the equation, the coefficients of the differential pressure function for a purely sinusoidal flow rate $Q(t) = Q_{max}sin(\omega t)$ are calculated and converted in the form $\Delta p_u(t) = A_u \sin(t \cdot St + \epsilon)$, where A_u is the amplitude of the unsteady solution and ϵ is the phase shift with respect to the volumetric flow function. In the quasi-steady case, the volumetric flow rate is calculated at each time point using the formula derived from the actual pressure difference for the steady-state flow so that the pressure amplitude of the quasi-static solution is the pressure amplitude A_{st} associated with the volumetric flow Q_{max}. Then, the ratio of the transient and quasi-static pressure amplitudes A_u/A_{st} (similar to the phase shift $_epsilon$) depends only on the number Wo and can therefore be plotted as a function of the number Wo, as shown in Figure 4.

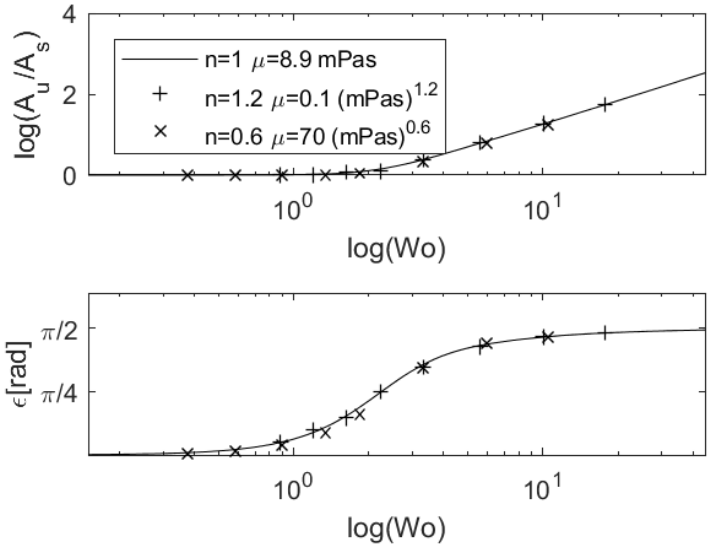

Figure 4: (Upper panel) Amplification diagram. (Lower panel) Phase shift between flow rate and pressure difference. In both panels, solid line depicts the analytical solution and circles are the CFD results for power-law fluid.

3.2 Extension to power law liquid

In the case of a power-law liquid, the governing partial differential equation is nonlinear, which solution is cumbersome. For this reason, transient CFD simulations with deformable mesh were performed, where the harmonic motion of the piston generates the periodic volume flow rate. The simulations were run for Newtonian and power-law fluids. During the evaluation, it was found that the the dimensionless Wo Womersley number can characterise well the effect of excitation frequency. For small Womersley numbers, the quasi-stationary solution estimates the transient result with reasonable accuracy, while for large Wo, the approximation is poor.

Figure 4 shows the amplification diagram of the analytical Newtonian case (continuous) and the values obtained from CFD simulations for Newtonian (n=1) and power-law fluids (n≠1). For a power-law fluid, the Wo Womersley number was calculated using the corrected formula. The figure proves that the Newtonian results are usable for the power-law case using the corrected Reynolds number. On the other hand, the discrepancy between the transient and steady-state approaches becomes significant at about Wo=1. At Wo=10, the volume flow rate and the pressure difference are completely out of phase. As a result, it can be said that for Wo<1, the quasi-static approximation can be applied with reasonable accuracy.

Thesis 3

The hysteresis in the damping characteristic $F(v)$ of power law ($\tau = K\dot{\gamma}^n$) liquid-filled damper with an annular gap shaped restriction during a periodic motion appears in the

$$Wo = \sqrt{2StRe_{korr}} > 1$$

region, where Wo is Womersley number, Re_{korr} is the generalised reynolds number for power law liquid in the critical cross section and St is the Strouhal number:

$$Re_{korr} = \frac{\rho U^{2-n} h^n}{K\left(\frac{0{,}5+n}{n}\right)^n}, \quad St = \frac{\omega h}{U}.$$

A quasi-stationary solution with $Wo < 1$, $Re_{korr} < 10$, $0.6 \leq n \leq 1.3$, results maximum error of 5% compared to the transient CFD solution.

The quantities in the above presented formulas are the angular frequency of the excitation ω, the amplitude of the velocity v_{max}. h is the half-width of the gap ring, D is the diameter of the piston, $U = v_{max}\frac{A_{\text{piston}}}{A_{\text{gap}}} = v_{max}\frac{D}{4h}$ is the maximum average velocity in the gap. ρ is the density of the fluid, K is the flow consistency index and n is the flow behavior index.

Related publication: [C1].

4 Design of the adjuster

Figure T4 shows a schematic drawing about the adjuster and its environment. The actuator consists of a cylinder (grey) and a piston connected to the adjuster's piston (green). The actuator piston can move in the adjuster cylinder (yellow), causing the fluid to flow through a gap with external diameter d_o, internal diameter d_i and length L. Since the liquid is incompressible, the spring-loaded compensating piston (blue) is necessary to compensate for the difference in volume change between the two chambers. The adjuster connects to the clutch spring.

During a speed shift, the load valves of the upper cylinder (grey) open and the actuator pressure p_{cyl} increases to 8 bar. This forces the adjuster (green and yellow) to move and compress the clutch spring. The pressure in the lower chamber of the adjuster increases; hence the fluid starts to flow into the upper chamber, and the adjuster compresses. In the released state, the upper pressure of the adjuster will be higher than the lower chamber pressure because of the compressed spring connected to the compensator piston. The fluid flows back from the upper chamber to the lower cavity. If wear has occurred, the balance between the compensating spring and the actuator spring will shift, allowing the adjuster to change length further.

The geometry of the adjuster is described by 5 dimensions: d_o gap outer diameter, d_i gap inner diameter, L gap length, D_d lower cylinder diameter and D_u upper cylinder diameter. The design process aims to determine these five dimensions and the applied fluid. I performed a multiobjective optimization for different shear thickening rheologies to achieve the best solution for these five dimensions. Based on the results, the design engineers would determine the dimensions to satisfy the requirements. The final product can be designed based on additional considerations (manufacturing technology, economics) from the resulting combinations.

4.1 Multiobjective optimisation

The adjuster has two main functions: 1) to be sufficiently rigid during operation, and 2) to compensate for the dead volume change, which is the sum of compression and wear during operation. If the restriction is too narrow or the fluid too viscous, the adjuster will be very stiff during actuation but not flexible enough during the adjustment period. On the other hand, the adjuster will be too flexible during operation if the restriction is too large or the fluid too "soft". Therefore, a compromise between these two objectives must be made.

For optimization, two independent objective functions are defined. In the first case, the cylinder pressure p_cyl is increased to 8 bar using a linear unit jump function and the compression o_1 over 2 s is defined as the first objective function. In the second case, the cylinder pressure was kept constant at atmospheric pressure, and the wear was changed by 0.5 mm. The length of the not adjusted wear o_2 during the 20s is defined as the second objective function. These two objectives (o_1, o_2) are minimized with the multiobjective optimization for different rheological fluids.

The behaviour of the device in the application environment is described by a system of ordinary differential equations (KDE) with 6 degrees of freedom, derived from the equations of motion for each component. The effect of the non-Newtonian fluid was taken into account by the $F(v)$ function presented earlier. The accuracy of the results was verified using time-dependent CFD simulations.

4.2 Contrains

The CFD results showed that the analytically calculated characteristic curve has reasonable accuracy for large relative L/h gap lengths. Although the results showed that the sensitivity of the relative gap size h/d is negligible, I still imposed is based on literature studies (e.g. [11]). I arbitrarily set $L/h < 100$ and $h/d_o < 0.1$.

In addition to practical considerations, the numerical scheme of the ordinary differential equation solver limits the range of design variables. The condition number of the governing differential equation system and the type of the corresponding numerical solver are strongly influenced by the flow model. In the case of small pressure loss (small choking and/or low viscosity fluid) the adjuster can suddenly compress which requires conventional (e.g., *ode23*, *ode45*) solvers, e.g., 4-5. Runge-Kutta-Fehlberg method. However, for large pressure losses (small gap and/or high viscosity fluid), the compression of the adjuster is minimal (in the nanometer range, three orders of magnitude smaller than the actuation length of 20 mm), requiring the use of rigid solvers. Moreover, the descriptive KDE equations have to be solved not only a few times but thousands of times during the optimization for different condition numbers. To handle this problem, additional nonlinear constraints have been introduced to exclude a parameter range that is not relevant for the application. Thus, it is sufficient to use only a rigid solver (e.g. *ode23s*).

With the analytical methods presented earlier, one can determine the force - velocity characteristic $F(v)$ for a given fluid and geometry. For a given fluid, the shape of this curve does not change as the dimensions are varied, but the position of the curve in the $F - v$ plane (Figure T4) can vary over a wide range. In Figure T4, I have plotted the characteristic forces on the $F(v)$ plane corresponding to the actuation ($F_{crit,2}$= 6000 N) and the adjustment ($F_{crit,2}$= 10 N). The characteristic velocities were defined with the industrial partner: the maximum compression velocity at actuation is $v_{crit,2} = 10^{-5}$ m/s, while the minimum velocity during the adjustment is $v_{crit,1} = 10^{-7}$ m/s. If the gap is too small, a large force is obtained (Figure T4 g) even at lower speeds than the minimum, resulting in a very stiff adjuster throughout the whole process, and the adjustment will not be achieved. If the gap is too large, then only high forces are obtained for speeds higher than the allowable maximum (Figure T4 h), in which case the adjuster will be continuously compressed at a high load, which is detrimental during the actuation phase. The thickening region of the curve may be in the middle-velocity range (Figure T4 a-e). In this case, if the adjuster is operating in the hardened third region (blue dotted line) during the process, we will not exploit the middle hardening section (Figure T4 a). The situation is similar if the adjuster operates on the soft section (dashed in Figure T4 f).

It can be concluded based on the above presented reasons that the appropriate design

are that make the hardening region of the curve $F(v)$ fall within the rectangle spanned by the points $v_{crit,1}, F_{crit,1})$ and $v_{crit,2}, F_{crit,2})$. The optimization results confirmed this: we obtained only appropriate geometric size combinations that met this sufficient condition.

4.3 Results

The results corresponding to the different rheologies are plotted as Pareto fronts. The Pareto points were classified into arbitrarily chosen quality classes. The results showed that several points were obtained for two liquids satisfying the industrial requirements.

On the other hand, the investigated fluids have different rheological properties, e.g. a) different $\mu(\dot{\gamma} = 1)$ zero-point viscosities, b) different critical shear rates where the shear thickening effect starts, and c) different hardening properties (ratio of minimum to maximum viscosity). Therefore general guidelines could be formulated to help the fluid selection. The results showed that the geometric dimensions could compensate for the effect of zero viscosity and critical shear rate but not the rate of thickening. Consequently, a fluid with a high shear thickening rate would be an optional choice for an adjuster.

Thesis 4.

Using a shear hardening fluid, a passive (no external energy source required) clutch actuator can be implemented that meets the usual requirements:

a) maximum Δx compression in case of actuating force F_{akt} over time t_{akt}, and

b) adjusting Δw wear in the released state over time t_u.

Let the annular gap L long in a piston adjuster with cross section $A = D^2\pi/4$ and let $W = \frac{d_o+d_i}{2}2\pi$ be the circumference of the annulus, s the stiffness of the spring in the actuator. Let $F_u = s\,\Delta w$ denote the spring force caused by the wear Δw. Then the design steps are:

1. Determination of the rheological curve of the applied fluid $\tau(\dot{\gamma})$ and the points A and B corresponding to the minimum and maximum viscosities, see panel (a) in Figure T4. (The thickening region is located between points A and B.)

2. Determination of the relative characteristic curve $\tilde{Q}(\tau)$ of the flow restriction in the adjuster (panel b of Figure T4) from the inverse rheological curve $\dot{\gamma}(\tau)$

$$\tilde{Q}(\tau) = \frac{1}{\tau^2}\left(2\tau\mathcal{F}(\tau) - 2\mathcal{S}(\tau)\right), \quad \text{where} \quad \mathcal{F}(\tau) = \int \dot{\gamma}(\tau)\,d\tau, \quad \mathcal{S}(\tau) = \int \mathcal{F}(\tau)\,d\tau.$$

3. Formulation and plotting of the force-velocity curve $F(v)$ using the following formulas

$$F = \tau\frac{L}{h}A, \quad v = \tilde{Q}(\tau)\frac{Wh^2}{A}$$

4. Calculation of the forces $F_A = \tau_{\mu,min}\frac{L}{h}A$ and $F_B = \tau_{\mu,max}\frac{L}{h}A$, finally add the rectangle defined by the points $(v_{min}, s\,\Delta w)$ and (v_{max}, F_{akt}).

The sufficient condition for the operability is that only the hardening section of the force characteristic $F(v)$ between points A and B falls within the rectangle defined in the previous step, i.e. the conditions $v_{min} \leq v_{A,B} \leq v_{max}$, $F_A < F_u$ and $F_B > F_{akt}$ are satisfied, see panel c) of Figure T4.

No geometric data are needed to perform the calculations described in items 1. and 2., only the rheological curve of the fluid to be used.

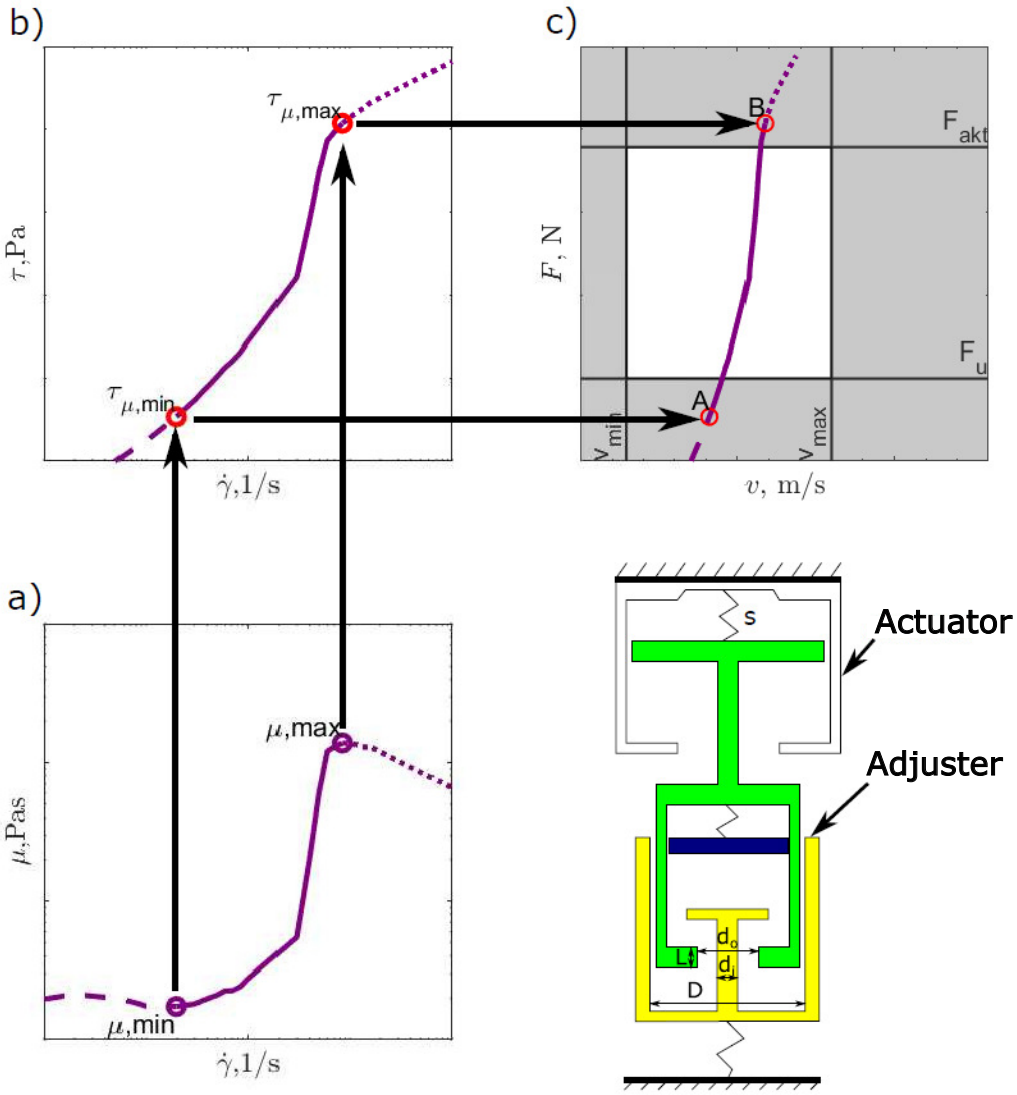

Figure T4. Explanation for Thesis 4.

Related publication: [J3].

5 Verification measurements

Although the more accurate numerical (CFD) simulations verified the analytical models, for a practical application, experimental verification is essential. To validate the models, I built an experimental setup to measure the differential pressure-volume flow characteristic curves of two types (annular ring, cylindrical hole) and different gap sizes for non-Newtonian fluid.

During the measurements, an actuator pushed the adjuster, and the built-in position sensor measured the compression as a function of time. A force sensor was inserted between the actuator and the adjuster device to record the compression force. From the position signal, the compression velocity was produced applying the Savitzky-Golay filter and compared the analytical and measured results for a given geometry in the form of force (velocity) curves $F(v)$. Results for the same fluid but different rheologies were compared using the relative characteristic curve (7).

The measurements were performed with three different types of fluid. First, Newtonian gear oil then conventional non-Newtonian (Cross) silicone oil of different viscosities were chosen. In the third case, the adjuster was filled with polypropylene-glycol silica nanoparticle suspension produced by the Soft Materials Research Group of the Faculty of Soft Materials, BME VBK. The shear thickening fluid was prepared with two types of silica particles.

The rheology of the fluids was highly temperature-dependent, so the Soft Materials research group measured the rheologies at different temperatures (20,25,30,40,55,70°C). Since it was impossible to keep the temperature constant in the laboratory, the analytical results compared with the measured data were calculated with the rheologies at 20, 25 and 30°C.

Figure 5 shows some typical results of the comparisons. Points in different colours correspond to different measurements, while black lines correspond to the analytical curves: 20°C-dotted, 25°C-solid, 30°C-sagged). The measurement points fell between the analytical curves, so the models can be considered reliable.

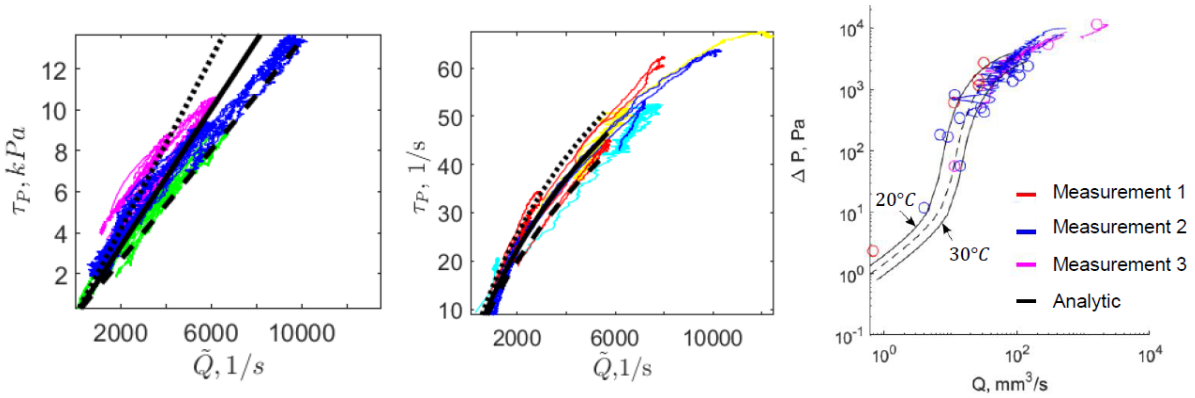

Figure 5: Typical measurement results for Newtonian (left), cross (middle) and shear thickening fluid (right) compared to analytical results (black).

6 Summary

The doctoral research aims to design a non-Newtonian fluid-based adjuster device that is rigid under high loads and flexible under low loads. The solution involves first developing an analytical model to model the flow of shear thickening fluid within the device. The simplified model with low computational cost was validated by more accurate numerical simulations in steady-state and transient cases, thus defining the limits of applicability of the model. Finally, I coupled the flow model with a system of equations of motion describing the device's behaviour and determined the required fluid and geometric dimensions by means of a multi-objective optimization. The validity of the models was also verified empirically.

Publications

Journal articles

[J1] **Nagy-György, Péter**, Dr. Hős Csaba, A Graphical Technique for Solving the Couette-Poiseuille Problem for Generalized Newtonian Fluids, *Periodica Polytechnica Chemical Engineering*, 63(1), 2019, doi: 10.3311/PPch.11817, IF(2020): 1.680

[J2] **Nagy-György, Péter**, Dr. Hős Csaba: Predicting the damping characteristics of vibration dampers employing generalized shear thickening fluids, *Journal of Sound and Vibration*, 506, 2021, doi: 10.1016/j.jsv.2021.116116, IF(2021): 3.655

[J3] **Nagy-György, Péter**, Dr. Bene József Gergely, Dr. Hős Csaba: An optimization-based design approach for a novel self-adjuster using shear thickening fluid. *Structural and Multidisiplinary Optimization*, 64(6):4161-4179, 2021, doi: 10.1007/s00158-021-03043-6, IF(2021): 4.542

Conference papers

[C1] **Nagy-György Péter**, Dr. Hős Csaba: Couette-Poiseuille flow of a General non-Newtonian Liquid in a Cylinder Annuli, *Conference on Modelling Fluid Flow*, Budapest, 2018. 9. 4. - 2019. 9. 7., (2018)

[C2] **Nagy-György Péter**, Dr. Hős Csaba: Nemnewtoni folyadékok alkalmazása lengéscsillapítókban, In: Barabás, István (szerk.) *XXIX. Nemzetközi Gépészeti Konferencia OGÉT 2021* Kolozsvár, Románia : Erdélyi Magyar Műszaki Tudományos Társaság (EMT) (2021) pp. 64-67. , 4 p.

[C3] Mayer Denise, **Nagy-György Péter**: Résáramlást leíró modell pontossági határainak meghatározása nemnewtoni közegek esetén In: Barabás, István (szerk.) *XXIX. Nemzetközi Gépészeti Konferencia OGÉT 2021* Kolozsvár, Románia : Erdélyi Magyar Műszaki Tudományos Társaság (EMT) (2021) pp. 56-59. , 4 p.

[C4] **Nagy-György Péter**; Hős Csaba: Pneumatikus munkahenger rugókarakterisztikájának mérése In: Barabás, István (szerk.) *XXVII. Nemzetközi Gépészeti Konferencia OGÉT 2019* Nagyvárad, Románia : Erdélyi Magyar Műszaki Tudományos Társaság (EMT) (2019) 632 p. pp. 376-379. , 4 p.

[C5] **Nagy-György Péter**, Dr. Hős Csaba: Hidraulikus munkahenger modellezése nemlineáris terhelés és csúszómód szabályozás esetén, Marosvásárhely, Románia, *2018, XXVI. Nemzetközi Gépészeti Konferencia: OGÉT 2018* (Csibi, Vencel-József; Barabás, István), Marosvásárhely, Románia, pp. 317-320. , 4 p.

References

[1] H. H. Solberg, *Self-adjusting clutch actuator for operating a vehicle clutch*, 2011.

[2] K. T. LJØSNE, *Automatically adjusting clutch actuator*, 2015.

[3] S. Tsangaris, C. Nikas, G. Tsangaris, and P. Neofytou, "Couette flow of a bingham plastic in a channel with equally porous parallel walls," *Journal of Non-Newtonian Fluid Mechanics*, vol. 144, no. 1, pp. 42–48, 2007.

[4] S. Hong, N. Wereley, Y. Choi, and S. Choi, "Analytical and experimental validation of a nondimensional bingham model for mixed-mode magnetorheological dampers," *Journal of Sound and Vibration*, vol. 312, no. 3, pp. 399–417, 2008.

[5] G. Zhang, Y. Wang, and J. Ma, "Bingham plastic fluid flow model for ceramic tape casting," *Materials Science and Engineering: A*, vol. 337, no. 1-2, pp. 274–280, 2002.

[6] K. Lin, H. Liu, M. Wei, A. Zhou, and F. Bu, "Dynamic performance of shear-thickening fluid damper under long-term cyclic loads," *Smart Materials and Structures*, vol. 28, no. 2, p. 025007, 2018.

[7] M. Wei, K. Lin, and H. Liu, "Experimental investigation on hysteretic behavior of a shear thickening fluid damper," *Structural Control and Health Monitoring*, p. e2389, 2019.

[8] D. Das and J. Arakeri, "Unsteady laminar duct flow with a given volume flow rate variation," *J. Appl. Mech.*, vol. 67, no. 2, pp. 274–281, 2000.

[9] C.-I. Chen, Y.-T. Yang, *et al.*, "Unsteady unidirectional flow of bingham fluid between parallel plates with different given volume flow rate conditions," *Applied Mathematical Modelling*, vol. 28, no. 8, pp. 697–709, 2004.

[10] Q.-H. Nguyen and S.-B. Choi, "Dynamic modeling of an electrorheological damper considering the unsteady behavior of electrorheological fluid flow," *Smart materials and structures*, vol. 18, no. 5, p. 055016, 2009.

[11] P. Filip and J. David, "Applicability of the limiting cases for axial annular flow of power-law fluids," *Recent Advances in Electrical Engineering Series*, vol. 12, pp. 45–48, 2013.